Improving the operation temperature of semiconductor-based Terahertz photodetectors: A multiphoton design

AIP | Applied Physics Letters

Improving the operation temperature of semiconductor-based terahertz photodetectors: A multiphoton design

Fabrizio Castellano, Rita C. Iotti, and Fausto Rossi

Citation: Appl. Phys. Lett. **92**, 091108 (2008); doi: 10.1063/1.2890167
View online: http://dx.doi.org/10.1063/1.2890167
View Table of Contents: http://apl.aip.org/resource/1/APPLAB/v92/i9
Published by the American Institute of Physics.

Improving the operation temperature of semiconductor-based terahertz photodetectors: A multiphoton design

Fabrizio Castellano,[1,a)] Rita C. Iotti,[1] and Fausto Rossi[1]
[1]*Dipartimento di Fisica, Politecnico di Torino, Corso Duca degli Abruzzi 24, 10129 Torino, Italy*

(Received 15 January 2008; accepted 11 February 2008; published online 4 March 2008)

We propose and theoretically investigate a semiconductor-based terahertz-detector design exploiting a multiphoton absorption strategy through a bound-to-bound-to-continuum scheme. Our results demonstrate that such a multisubband architecture may access values of the background-limited infrared photodetection temperature, significantly higher than those of conventional quantum well infrared photodetectors operating at the same frequency, and therefore could represent a better alternative to the latter in the terahertz spectral region. © *2008 American Institute of Physics*. [DOI: 10.1063/1.2890167]

The extremely high-potential applications of sensors and detectors operating in the terahertz region of the electromagnetic spectrum justifies the intensive research activity carried out in the past years. In particular, that for devices compatible with state-of-the-art semiconductor micro- and optoelectronic architectures is the ultimate quest. Several threads may be identified in the latter. Broad-spectrum terahertz detection has been achieved by means of heterojunction interfacial work function internal photoemission devices.[1–3] Plasmon-resonance field effect transistors designs for terahertz and subterahertz detections have been experimentally demonstrated.[4–6] Devices based on ions trapped inside carbon nanotubes have also been theoretically proposed both as detectors and emitters of terahertz radiation.[7] Devices exploiting the quantum hall effect have been recently studied for their short response time and spectral selectivity.[8,9] Quantum-cascade structures, which have been shown to efficiently operate as detectors at high temperatures in the mid-infrared (mid-IR) range,[10] are currently being extended into the terahertz regime.[11] Also, detection techniques exploiting the electro-optical effects in $LiTaO_3$, $LiNbO_3$, and ZnTe crystals, such as phase retardation of pulsed terahertz probes[12] or coherent upconversion of the terahertz field,[13] have been proposed.

As discussed also in Ref. 14 one of the most promising directions appears to be the one indicated by quantum well infrared photodetectors (QWIPs).[15] While that of mid-IR QWIPs is a well established technology, its extension into the far-IR (terahertz) range is still at an initial development stage. Indeed, one of the main issues in terahertz-operating QWIPs is the huge dark current value that causes the background limited infrared photodetection temperature (T_{blip}) of terahertz QWIPs to lie in the range of 10–15 K,[16,17] i.e., much lower than that of state-of-the-art mid-IR devices.

The principle of operation of conventional QWIPs resorts on electronic transitions, induced by the incident radiation, from the single bound state of each quantum well directly into the continuum band. State-of-the-art QWIPs operating in the mid-IR spectral region efficiently exploit this architecture and show remarkable levels of performance.[15]

Recently, the use of multilevel architectures, opening up to bound-to-bound electronic transitions, has been proposed and studied, focusing both on their intrinsic nonlinear character and on their wide-band absorption spectra. While the latter feature allows for multi-color[18] or wideband detection,[19–22] second-order nonlinearities of two-level systems have been studied and experimentally demonstrated with the idea of using the devices for second-order autocorrelation measurements.[23–26]

In a previous work,[14] we theoretically addressed the advantages deriving from the application of a multilevel architecture in terahertz QWIP designs. In particular, we concluded that the latter, through a bound-to-bound-to-continuum multiphoton absorption scheme, may efficiently face the above-mentioned dark current problem.

In the present letter, we shall quantitatively investigate the performances of such a scheme, referring to a specific figure of merit of QWIPs, namely, the T_{blip}. The latter is defined as the temperature at which the current due to thermal noise in the device (dark current) equals the current induced by the 300 K background (background photocurrent). To properly evaluate these quantities, we shall extend and improve the model presented in Ref. 14 by considering the incident radiation as due to a 300 K blackbody source corresponding to the detection background.

Our prototypical device consists of an infinitely periodic heterostructure supporting, within each period, a set of equally spaced bound states. This may be achieved by diverse design strategies. In particular, in the present paper, we are considering nested-quantum-well structures, which are alternative to the multi-quantum-well scheme proposed in Ref. 14. The nested-quantum-well strategy can be easily handled to increase the number of equally spaced bound states; to this end, the potential-profile envelope should resemble a parabola, which would ultimately be the ideal choice. Figure 1 shows the potential profile along the growth direction for the case of a four-subband device. In the following, results will be presented for the latter as well as for similar structures supporting one, two and three subbands.

In our fully tridimensional model, the supercell shown in Fig. 1 is infinitely replicated along the growth direction. Such a repetition of the basic unit is indeed the strategy exploited in these unipolar devices to optimize detection efficiency. Finite-size (i.e., boundary and contact) effects are therefore of minor importance and are neglected in this work as well as in-plane confinement.

[a)]Electronic mail: fabrizio.castellano@polito.it

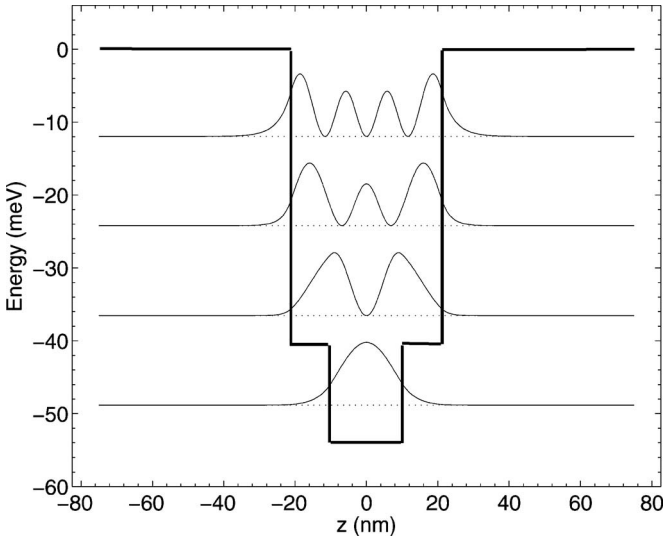

FIG. 1. Potential profile along the growth direction of our prototypical bound-to-bound-to-continuum device. In particular, the symmetric nested-quantum-well structure has four geometric parameters that can be varied to tune the position of up to four bound levels. The interlevel separation corresponds to a detection frequency of 3 THz.

The band structure of our prototypical device is obtained within the usual envelope-function scheme. In particular, the electron in-plane dispersion relation is assumed to be purely parabolic, while the band structure along the growth direction is computed from the Schrödinger equation projected along the z direction by means of a plane-wave expansion.[27] Due to the typically low doping levels in this kind of devices, charge-density effects on the potential profile may safely be neglected and no Schrödinger–Poisson coupling is included in our modeling.

The transport model employed to describe the steady-state electron dynamics in our unipolar device is based on the Boltzmann transport equation describing the distribution of electrons in the conduction band. Its general form for the case in which the latter is split into N subbands is the following:

$$\frac{e}{\hbar}\mathbf{F}\cdot\nabla_{\mathbf{k}}f_{\mathbf{k}i}+\sum_{\mathbf{k}'j}\left(P_{\mathbf{k}i,\mathbf{k}'j}f_{\mathbf{k}'j}-P_{\mathbf{k}'j,\mathbf{k}i}f_{\mathbf{k}i}\right)=0, \tag{1}$$

where $f_{\mathbf{k}i}$ is the distribution function of a state in subband i with wave vector $\mathbf{k}$. In the following, a single label α will be used to denote the pair $(\mathbf{k},i)$. The electron drift term is due to the external electric field $\mathbf{F}$. Although the latter may in general be oriented in any direction, in the present paper, we will limit our discussion to biases applied only along the growth axis.

The quantities $P_{\alpha\alpha'}$ in Eq. (1) are the probabilities per unit time that a scattering event bringing an electron from a state α' to a state α occurs. They correspond, in principle, to all possible interaction mechanisms affecting the electron dynamics (electron-photon, electron-phonon, electron-electron, etc.). Since the aim of the present paper is to focus on the electron-photon interaction, the latter will be treated in a fully microscopic scheme by use of the Fermi's golden rule. Conversely, all other interactions will be described in terms of a phenomenological electronic mean lifetime τ guaranteeing the proper thermalization of the electron population in the absence of external electromagnetic fields. Such a mean lifetime therefore enters the model as a fitting parameter, representing the global strength of all nonradiative thermalization mechanisms.

As mentioned above, to evaluate the T_{blip} of our prototypical detector, we have to study its interaction with the background radiation, considered as due to a blackbody source at 300 K. In particular, to properly describe the latter, we employ a fully quantum mechanical treatment of the electromagnetic field. More specifically, the electron-photon interaction hamiltonian operator is

$$\hat{H}^{\text{opt}}=\sum_{\alpha\alpha'\mathbf{q}}\left[g_{\alpha\alpha'\mathbf{q}}\hat{c}^{\dagger}_{\alpha}\hat{a}_{\mathbf{q}}\hat{c}_{\alpha'}+g^{*}_{\alpha\alpha'\mathbf{q}}\hat{c}^{\dagger}_{\alpha'}\hat{a}^{\dagger}_{\mathbf{q}}\hat{c}_{\alpha}\right], \tag{2}$$

where the fermionic operator $\hat{c}^{\dagger}_{\alpha}$ ($\hat{c}_{\alpha}$) denotes the creation (destruction) of a carrier in the single particle state α, while the bosonic operator $\hat{a}^{\dagger}_{\mathbf{q}}$ ($\hat{a}_{\mathbf{q}}$) denotes the creation (destruction) of a photon with wave vector $\mathbf{q}$. The first (second) contribution in Eq. (2) describes a process in which an electron performs a transition between the two single-particle states, α and α', absorbing (emitting) a photon; this mechanism has a coupling constant $g_{\alpha\alpha'\mathbf{q}}$ which is expressed as

$$g_{\alpha\alpha'\mathbf{q}}=\frac{i\hbar e}{m\sqrt{2}}\mathbf{A}_{\mathbf{q}}\cdot\mathbf{p}_{\alpha\alpha'}, \tag{3}$$

where $\mathbf{p}_{\alpha\alpha'}$ is the momentum matrix element between states α and α' and $\mathbf{A}_{\mathbf{q}}$ is the electromagnetic field vector potential component with wavevector $\mathbf{q}$, whose absolute value can be computed from the spectral energy density of the blackbody radiation.

The probability per unit time $P^{\text{opt}}_{\alpha\alpha'\mathbf{q}}$ of an electron-photon scattering event is then computed using Fermi's golden rule

$$P^{\text{opt}}_{\alpha\alpha'\mathbf{q}}=\frac{2\pi}{\hbar}|\langle\alpha,n_{\mathbf{q}}|H^{\text{opt}}|n'_{\mathbf{q}},\alpha'\rangle|^2\delta(E_{\alpha}-E_{\alpha'}\pm\hbar\omega_{\mathbf{q}}), \tag{4}$$

where the $+(-)$ sign refers to an emission (absorption) process, $\hbar\omega_{\mathbf{q}}$ is the photon energy, and $n_{\mathbf{q}}$ is the photon occupation number. The scattering probability for the electron subsystem is obtained from Eq. (4) by summing over all photon modes $\mathbf{q}$ and assuming $n_{\mathbf{q}}$ to be the Bose–Einstein distribution function. The calculation gives

$$P^{\text{opt}}_{\alpha\alpha'}=\frac{\mathcal{F}e^2\hbar\omega}{4\pi^2c^3m^2\varepsilon}|\mathbf{p}_{\alpha\alpha'}|^2\left(\frac{1}{e^{\hbar\omega/k_BT}-1}+\frac{1}{2}\pm\frac{1}{2}\right), \tag{5}$$

where $\hbar\omega$ is the energy difference between states α and α', $\mathcal{F}$ is the device field of view (FOV), ε is the dielectric constant, and T is the blackbody temperature. Equation (5) shows that electron-photon scattering probabilities are completely determined by the blackbody temperature and the device band structure, without resorting to external fitting parameters.

On the other hand, the modeling of thermal scattering mechanisms contains a free parameter τ which has to be modulated to fit with experimental findings. In particular, a reasonable choice is to adjust τ in order to reproduce the measured T_{blip} (12 K) of the bound-to-continuum QWIP operating at 3.2 THz, with a 90° FOV, and reported in Ref. 17. A T_{blip} of approximately 12 K is obtained for $\tau\approx 50-100$ ps. It is important to stress that this very large value derives from the fact that we are using a simplified

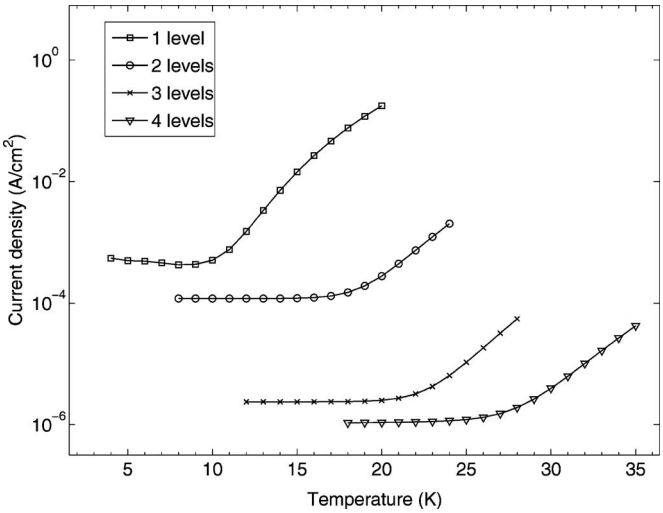

FIG. 2. Current density along the growth direction, as a function of device temperature, for four diverse multilevel designs differing in the number of bound states. The four-level curve corresponds to the design of Fig. 1.

model for thermal scattering; our fitting parameter τ is not to be taken as a realistic measure of electron scattering time in a real semiconductor.

Figure 2 shows the total currents obtained when our prototypical devices are exposed to a 300 K blackbody radiation and biased with a 50 V/cm electric field along the growth direction. Our calculations have been performed for the case of an electron density of 1×10^{17} cm^{-3}, which is a typical value for GaAs/AlGaAs based devices.[17] The value of τ has been set equal to 80 ps.

Each curve allows to identify a low-temperature regime in which the dark current is negligible with respect to the photocurrent: the total current is therefore independent from the device temperature. Conversely, in the high-temperature region, the dark current increases almost exponentially so that the photocurrent quickly becomes negligible and the current is totally dominated by the "dark" contribution. The significant decrease of the photocurrent for the diverse designs is mainly due to the reduction of the photoconductive gain. The latter, for the four level structure, gets down to just 0.2% of the value of one level QWIP, while the quantum efficiency is only lowered by 14%.

The dashed horizontal lines in Fig. 2 mark the current doubling and their interception with each of the curves identifies the T_{blip} of each device. It can be seen that the latter is shifted to higher values as the number of bound levels is increased. The diverse designs are found to exhibit values of T_{blip}=11.5, 19.5, 23.5, and 28.5 K for the cases of one, two, three, and four bound levels, respectively. The relevant increase of T_{blip} is justified by the fact that although both the photocurrent and the dark current decrease on increasing the number of bound levels, the latter decreases faster than the former and therefore the temperature at which the two are equal moves to higher values.

In summary, we have proposed and theoretically investigated a semiconductor-based terahertz-detector design exploiting a multiphoton absorption strategy. Our findings provide a clear demonstration that the proposed multisubband scheme allows for higher T_{blip} values with respect to conventional QWIP designs operating at the same frequency, and therefore could represent a better alternative for terahertz radiation detection technology.

[1] A. G. U. Perera, S. G. Matsik, B. Yaldiz, H. C. Liu, A. Shen, M. Gao, Z. R. Wasilewski, and M. Buchanan, Appl. Phys. Lett. **78**, 2241 (2001).
[2] S. G. Matsik, M. B. M. Rinzan, A. G. U. Perera, H. C. Liu, Z. R. Wasilewski, and M. Buchanan, Appl. Phys. Lett. **82**, 139 (2003).
[3] M. B. M. Rinzan, A. G. U. Perera, S. G. Matsik, H. C. Liu, Z. R. Wasilewski, and M. Buchanan, Appl. Phys. Lett. **86**, 071112 (2005).
[4] W. Knap, Y. Deng, S. Rumyantsev, J.-Q. Lü, M. S. Shur, C. A. Saylor, and L. C. Brunel, Appl. Phys. Lett. **80**, 3433 (2002).
[5] W. Knap, Y. Deng, S. Rumyantsev, and M. S. Shur, Appl. Phys. Lett. **81**, 4637 (2002).
[6] E. A. Shaner, M. Lee, M. C. Wanke, A. D. Grine, J. L. Reno, and S. J. Allen, Appl. Phys. Lett. **87**, 193507 (2005).
[7] D. Lu, D. Lee, U. Ravaioli, and K. Schulten, Phys. Rev. Lett. **95**, 246801 (2005).
[8] C. Stellmach, A. Hirsch, G. Nachtwei, Yu. B. Vasilyev, N. G. Kalugin, and G. Hein, Appl. Phys. Lett. **87**, 133504 (2005).
[9] C. Stellmach, G. Vasile, A. Hirsch, R. Bonk, Y. B. Vasilyev, G. Hein, C. R. Becker, and G. Nachtwei1, Phys. Rev. B **76**, 035341 (2007).
[10] D. Hofstetter, M. Beck, and J. Faist, Appl. Phys. Lett. **81**, 2683 (2002).
[11] M. Graf, G. Scalari, D. Hofstetter, J. Faist, H. Beere, E. Linfield, D. Ritchie, and G. Davies, Appl. Phys. Lett. **84**, 475 (2003).
[12] C. Winnewisser, P. Uhd Jepsen, M. Schall, V. Schyja, and H. Helm, Appl. Phys. Lett. **70**, 3069 (1997).
[13] A. Nahata, J. T. Yardley, and T. F. Heinz, Appl. Phys. Lett. **75**, 2524 (1999).
[14] F. Castellano, R. C. Iotti, and F. Rossi, Appl. Phys. Lett. **88**, 182111 (2006).
[15] See, e.g., H. C. Liu, in *Intersubband Transitions in Quantum Wells: Physics and Device Applications I*, Semiconductors and Semimetals, Vol. 62, edited by H. C. Liu and F. Capasso (Academic, San Diego, 2000), Chap. 3, pp. 126–196.
[16] H. C. Liu, C. Y. Song, A. J. SpringThorpe, and J. C. Cao, Appl. Phys. Lett. **84**, 4068 (2004).
[17] H. Luo, H. C. Liu, C. Y. Song, and Z. R. Wasilewski, Appl. Phys. Lett. **86**, 231103 (2005).
[18] A. Majumdar, K. K. Choi, J. L. Reno, and D. C. Tsui, Appl. Phys. Lett. **83**, 5130 (2003).
[19] S. V. Bandara, S. Gunapala, J. K. Liu, S. B. Rafol, C. J. Hill, D. Z. Y. Ting, J. M. Fastenau, and A. W. K. Liu, Appl. Phys. Lett. **86**, 151104 (2005).
[20] M. P. Touse, G. Karunasiri, K. R. Lanz, H. Li, and T. Mei, Appl. Phys. Lett. **86**, 093501 (2005).
[21] J. Li, K. K. Choi, J. F. Klem, J. L. Reno, and D. C. Tsui, Appl. Phys. Lett. **89**, 081128 (2006).
[22] W. Liu, D. H. Zhang, Z. M. Huang, and W. J. Fan, J. Appl. Phys. **101**, 033114 (2007).
[23] H. C. Liu, E. Dupont, and M. Ershov, J. Nonlinear Opt. Phys. Mater. **83**, 5130 (2003).
[24] H. Schneider, T. Maier, H. C. Liu, M. Walther, and P. Koidl, Opt. Lett. **30**, 287 (2004).
[25] T. Maier, H. Schneider, M. Walther, P. Koidl, and H. C. Liu, Appl. Phys. Lett. **84**, 5162 (2005).
[26] T. Maier, H. Schneider, H. C. Liu, M. Walther, and P. Koidl, Appl. Phys. Lett. **88**, 051117 (2006).
[27] S. Barbieri, F. Beltram, and F. Rossi, Phys. Rev. B **60**, 1953 (1999).